Cooper Union for the Advancement of Science and Art

Analysis of Boeing 747-800's Aerodynamics Using First Principles

ME-422: Fundamentals of Aerodynamics

Authors:
Khushant Khurana

Professor:
Professor Wooton

May 7, 2024

Contents

1 Motivation

Understanding aerodynamics is crucial for ensuring the safety and stability of aircraft during all phases of flight, from takeoff to landing. By studying aerodynamics of aircraft, engineers can optimize the aerodynamic design of wings, airfoil, fuselage, and other components; hence reducing drag, increasing lift, and improving fuel efficiency. Although this design is done through varied iterations of experiments, engineering calculations can be performed to estimate the characteristics of an aircraft. In this paper, the aerodynamics of Boeing 747-800 are studied using first principles and the results are compared to actual simulations from XFLR modelling software.

2 Dimensions Airfoil Characteristics

2.1 Airfoil

The most common airfoil used by Boeing is the "Boeing BACXXX Airfoil - Boeing Commercial Airplane Company BACXXX Energy Efficient Transport Program airfoil". The max thickness of the airfoil is 11.3 % and the max camber is 1.4 % at 15 % chord length. The normalized coordinates of the airfoil, derived from [1] are plotted in Figure 2.1.

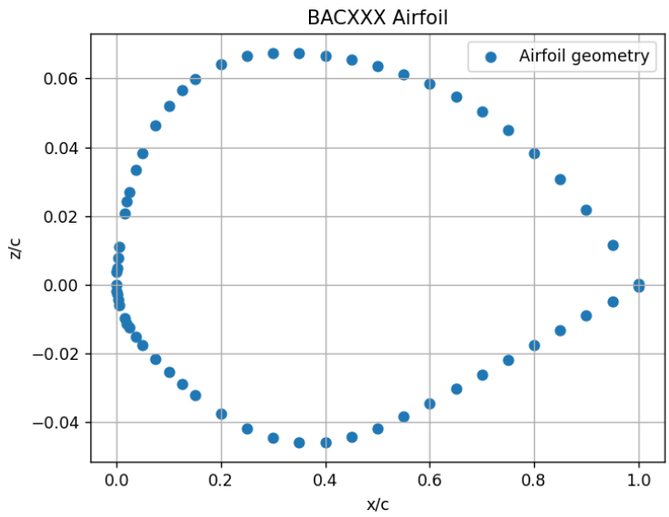

Figure 2.1: BACXXX Airfoil Coordinates

2.2 Geometric dimensions

Important characteristics of the Boeing 747-800 aircraft are found below:

Parameter	Magnitude
Root Chord	14.7 m [2]
Tip Chord	3.63 m [2]
Wingspan	68.58 m [3]
Twist	3 degree [4]
Wing Area	554 m^2 [3]
Aspect Ratio	6.97
Fuselage length	76.3 m [3]
Fuselage diameter	6.49 m [5]

Table 1: Boeing 747-800 Wing Geometric Characteristics

Parameter	Magnitude
Cruise Mach	0.86 [3]
Maximum Payload	447000 kg [3]
Takeoff speed	82.2 $\frac{m}{sec}$ [6]

Table 2: Boeing 747-800 Operating Conditions

2.3 Experimental Data

The section lift and drag coefficients for the Boeing BACXXX Airfoil are derived from Airfoil Tools [1]. Since most of the analysis will be conducted at steady state flight which has high speed and hence high reynolds number, the experimental data collected at high renolds number (5e6 - 10e6) is chosen. The corresponding relations between the coefficients and angle of attack are shown in Figure 2.2 and Figure 2.3.

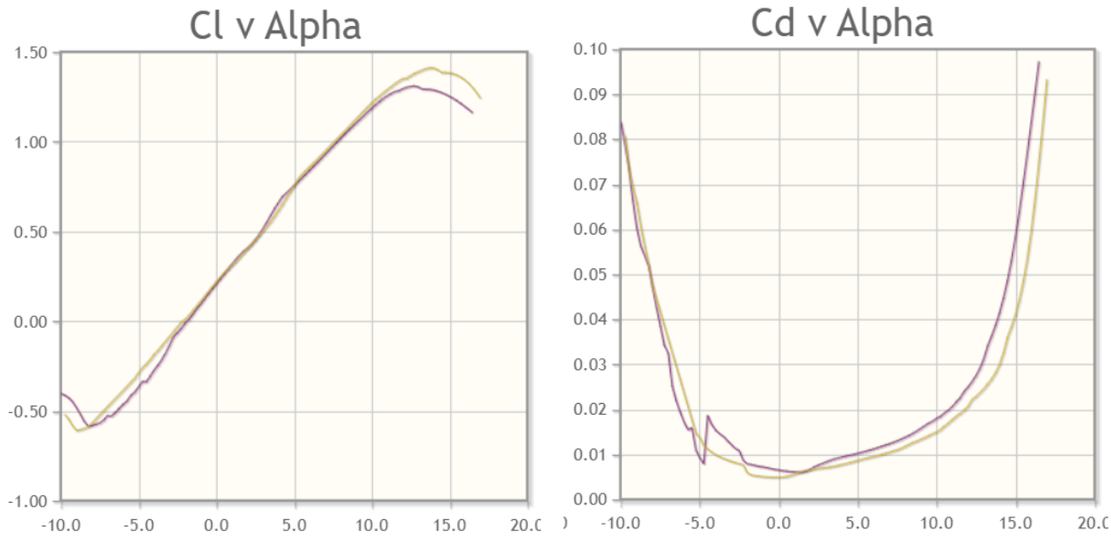

(a) Lift Coefficient

(b) Induced Drag Coefficient

Figure 2.2: High Reynolds number polar plots for BACXXX Airfoil (2)

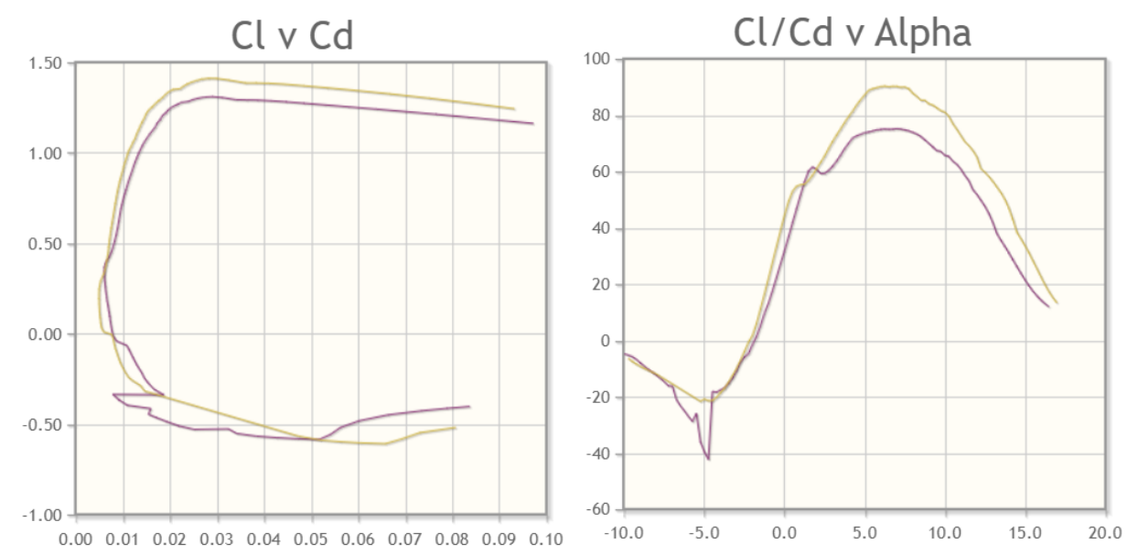

(a) $C_L as Function of C_D$

(b) The variation in $C_L/C_D as AO Avaries$

Figure 2.3: High Reynolds number polar plots for BACXXX Airfoil (2)

Besides the section non-dimensional coefficients, actual experimental data for Boeing 747-100, published by NASA Langley Center [7], is also regarded as a benchmark number. The data shows $C_L vs C_D$ measurements collected from a wind tunnel with Reynolds number = 1.8 e6 and center of gravity at 0.25 times the chord.

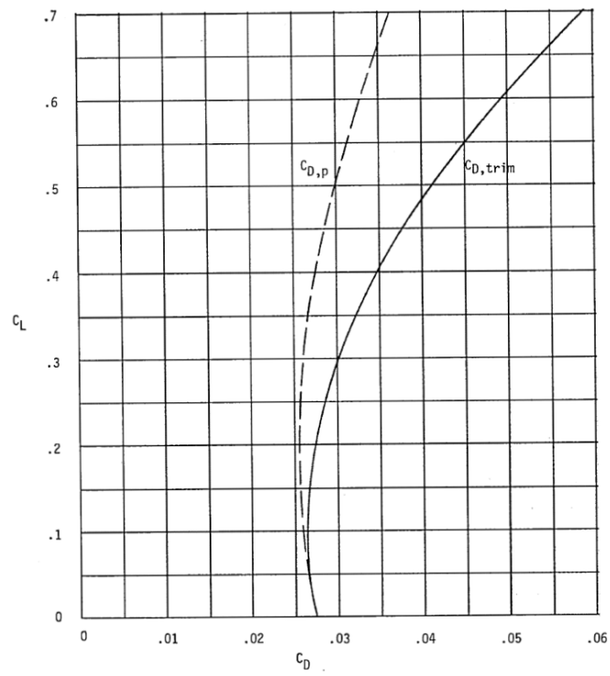

Figure 2.4: Wind tunnel trimmed lift - drag polar and estimated parasite drag coefficient; c.g. at 0.25 C; R = 1.08 x 10^6.

3 Thin Airfoil Theory Analysis (2D Analysis)

Thin airfoil theory assumes that the airfoil has a small thickness compared to its chord length (¡12%). This allows the airflow over the airfoil to be treated as two-dimensional, simplifying the analysis. Since the theory utilizes potential flow theory, it assumes the flow to be irrotational and inviscid. Moreover, the theory assumes a vortex sheet on the camber line which creates circulation and consequently lift, as explained by the Kutta Joukowski theorem in Equation 1

$$L' = \rho V_{\text{inf}} \Gamma \tag{1}$$

According to thin airfoil theory, the lift force and moments applied to a 2D airfoil can be determined using the change in camber line as shown in Equation 2 where σ is the vorticity strength over the camber line. In order to determine the camber line function of the BACXXX airfoil, 4 digit NACA convention is used as shown in Equation 3 where 'm' = maximum camber and 'p' = location of maximum camber.

$$\frac{1}{2\pi} \int_0^c \frac{\sigma(x_0)}{(x - x_0)} \, dx_0 = V_{\text{inf}}(\sin(\alpha) - \frac{dz}{dx} \cos(\alpha) \tag{2}$$

$$yc = \frac{m}{p^2}(2px - x^2), 0 \leq x \leq p. \tag{3}$$

$$yc = \frac{m}{(1-p)^2}((1 + 2p) + 2px - x^2), p \leq x \leq 1 \tag{4}$$

In order to integrate the vorticity strength function around the chord, Fourier coefficients are used to express the vorticity strength function as a $f(\theta)$as shown in Equation 5. The fourier coefficients are labelled as A_n and are determined using equations given in Equation 6

$$\sigma(\theta) = 2V_{\text{inf}}(A_0 \frac{1 + \cos(\theta)}{\sin(\theta)} + \sum_{i=1}^{n} A_n \sin(n\theta)) \tag{5}$$

$$A_0 = \alpha - \int_0^\pi \frac{dz}{dx} d\phi \tag{6}$$

$$A_n = \frac{2}{\pi} \int_0^\pi \frac{dz}{dx} (cos(n\phi) d\phi) \tag{7}$$

The coefficients are solved for cruise speed and the coefficient of lift and moment at the tip are determined as shown in Figure 3.1. The slope of the lift coefficient vs angle of attack is determined to be 6.28 which is approximately 2π and the angle of attack at $C_L = 0$ is -1.31 °. At cruise speed, the angel of attack is determined to be 0.5 degrees to generate lift force equaling the maximum payload of the aircraft.

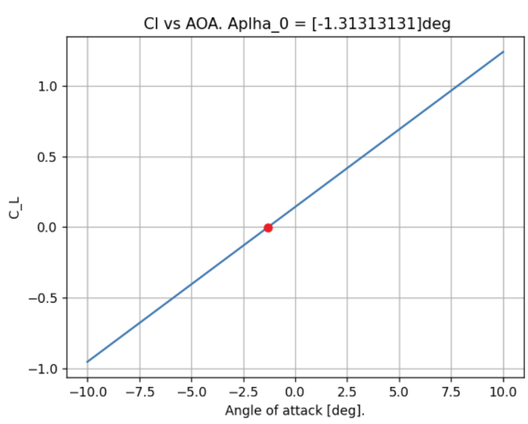

(a) Lift Coefficient

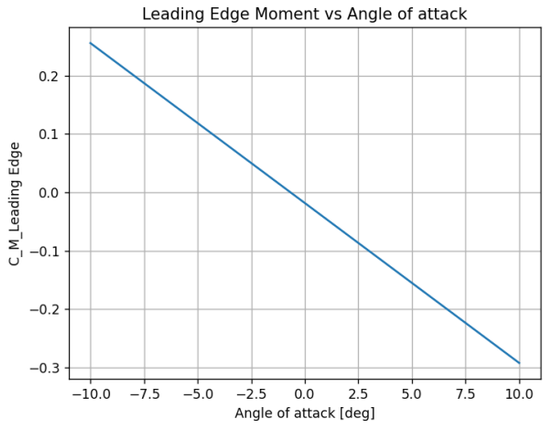

(b) Leading Edge Moment Coefficient

Figure 3.1: Thin Airfoil Theory Estimation

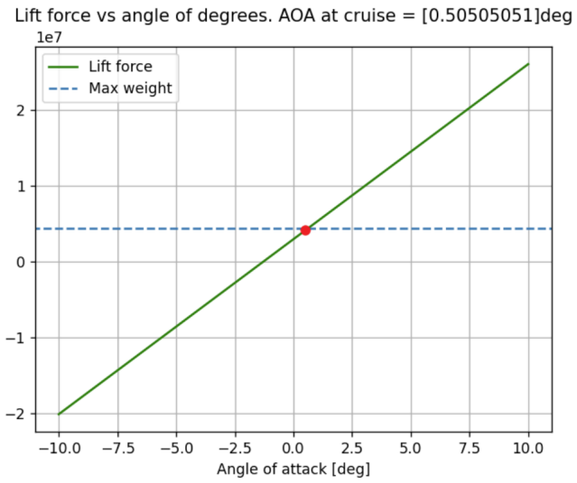

Figure 3.2: Angle of Attack at Steady State Flight

4 Finite Wing Theory Analysis (3D)

Since thin airfoil theory assumes a 2D profile and an infinite wing, it neglects effect of downwash. Downwash is the movement of the air from high pressure region underneath the wing to low pressure region top. Accordingly, there is no lift produced at the edges which results in a non-uniform vorticity distribution unlike the thin airfoil theory. To solve this problem, a parabolic distribution of vortex strength is considered which is 0 at the ends and peaks in the middle. The effect of downwash reduces the angle of attack as shown in Equation 8

$$\alpha_{\text{effective}} = \alpha - \alpha_{\text{induced}} \tag{8}$$

It was determined that the lift coefficient varies with angle of attack using the factor 2π. The magnitude of downwash is given using **??**. Putting this in context with the vorticity distrubtion function like before, the fundamental equation of finite wing theory is derived, Equation 10.

$$w(y_0) = \int_{-winspan/2}^{wingspan/2} \frac{\frac{d\Gamma}{dy}}{4\pi(y - y_0)} dy \tag{9}$$

$$\frac{\Gamma(y_0)}{\pi V_{\text{inf}} c(y_0} = \alpha(y_0) - \alpha_{\text{L-0}}(y_0) + \frac{1}{4\pi V_{\text{inf}}} \int_{-wingspan/2}^{wingspan/2} \frac{\frac{d\Gamma}{dy}}{4\pi(y - y_0)} dy \tag{10}$$

To solve the equation, the vorticity strength across the wing is assumed to be Fourier sum as shown in Equation 11. This transforms Equation 10 to Equation 12. The Fourier coefficients A_n are solved using linear system of equations: Ax = B. Using these coefficients, the lift and induced drag are determined as shown in Equation 13.

$$\Gamma(\theta) = 2bV_{\text{inf}} \sum_{i=1}^{n} A_n sin(n\theta) \tag{11}$$

$$\frac{2b}{\pi c(\theta)} \sum_{i=1}^{n} A_n sin(n\theta) + \sum_{i=1}^{n} nA_n \frac{sin(n\theta)}{sin(\theta)} = \alpha(\theta) - \alpha_{\text{L-0}}(\theta). \tag{12}$$

$$C_L = A_1 \pi (AspectRatio) \tag{13}$$

$$C_D = \frac{C_L^2}{\pi (AspectRatio)} (1 + \sigma) \tag{14}$$

The linear system of equations is solved in Python using 100 coefficients to generate precise values. The lift coefficient, induced drag coefficient, and the relations of the two are shown in Figure 4.1, and Figure 4.2. The modified lift coefficient, accounting for induced drag, has less slope than the 2D model which makes sense because the lift force is not uniform anymore. In other words, the downwash results in loss of lift force at the edges which introduces an induced angle of attack.

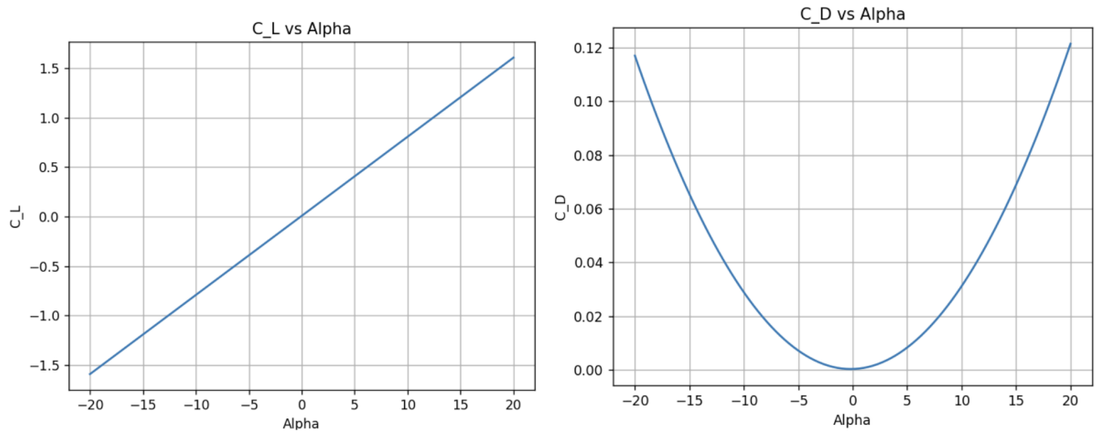

(a) Lift Coefficient

(b) Induced Drag Coefficient

Figure 4.1: Finite Wing Estimation (1)

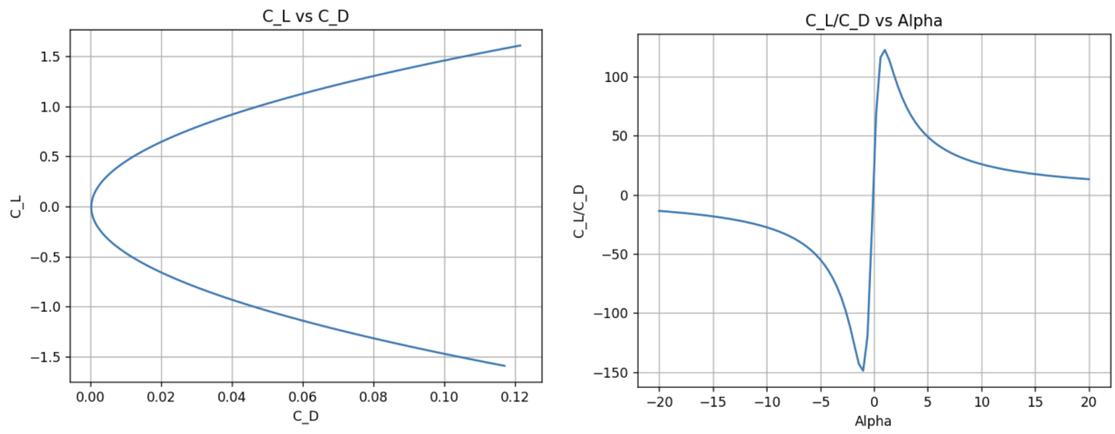

(a) $C_L as Function of C_D$

(b) The variation in $C_L/C_D as AO Avaries$

Figure 4.2: Finite Wing Estimation (2)

5 Viscous Model

Viscous effects in aerodynamics arise from skin friction due to boundary layers. Assuming no slip condition, the flow has 0 velocity at the contact surface which induces shear stress and gives rise to drag. Boundary layers can be classified as laminar and turbulent, based on the local Reynolds number. If the Reynolds number is greater than 3e5, critical Reynolds Number, the flow is considered to be turbulent.

5.1 Wing

The determination of skin drag on the wings of Boeing 747-800 is done using strip theory: the wing is split into multiple sections. Both laminar and turbulent effects are considered while analyzing individual strips and the shear force is determined using Equation 15. To make things easy, flat plate model is used to determine the drag force.

$$Drag_{\text{Laminar}} = 0.664 \rho V_{\text{inf}}^2 L (Re_L)^{\cdot} 5 \tag{15}$$

$$Drag_{\text{Turbulent}} = \frac{0.036 \rho V_{\text{inf}}^2 L}{Re^{\cdot} 2} \tag{16}$$

Since the incoming flow transitions from laminar to turbulent, the total drag on the section is determined using Prandtl Relation, shown in Equation 17

$$Drag_{\text{Total}} = Drag_{100\% \text{ Turbulent}} - Drag_{\text{Turbulent Where Laminar}} + Drag_{\text{Laminar}} \tag{17}$$

To calculate the total skin drag, 200000 sections are used and the final drag force is determined to be 605 kN and the coefficient of drag is 0.03 at steady state flight. The viscous drag is lies close to the induced drag for smaller angle of attacks (range of -10 to 10 degrees). However, with higher angle of attack, the induced drag coefficient increases.

5.2 Body: (Fuselage and Nose)

To analyze the viscous drag on the body itself, coefficient of drag over fundamental shapes is taken from [8]. Accordingly, the fuselage is considered as a long cylinder and the nose is considered as a hollow hemisphere. The corresponding coefficients are shown in Equation 18. The dimensions used for both shapes are given in Table 1. Like the wing analysis, steady level flight is assumed with conditions shown in Table 2.

$$C\_D_{\text{Fuselage}} = 0.86 \tag{18}$$

$$C\_D_{\text{Nose}} = 0.38 \tag{19}$$

Using the basic drag calculation, the overall drag is determined to be 1620 kN which seems to be a lot. However, if the entire body is considered as 1 shape - a stretched streamlined body - the coefficient of drag decreases to 0.04 [8]. Doing the same calculations, the total drag over the body equals to 53 kN which does make more sense.

6 XFLR5 Analysis (Software) & Stall Determination

The data points from the Airfoil Tools [1] for the BACXXX airfoil are entered into the XFLR5 software to validate the results found using fundamental methods and also determine stall characteristics. Reynolds number at cruise conditions (1.2e8) and angle of attack ranging from -25 to 25 degree are used for analysis. The results are shown in Figure 6.1 and Figure 6.2

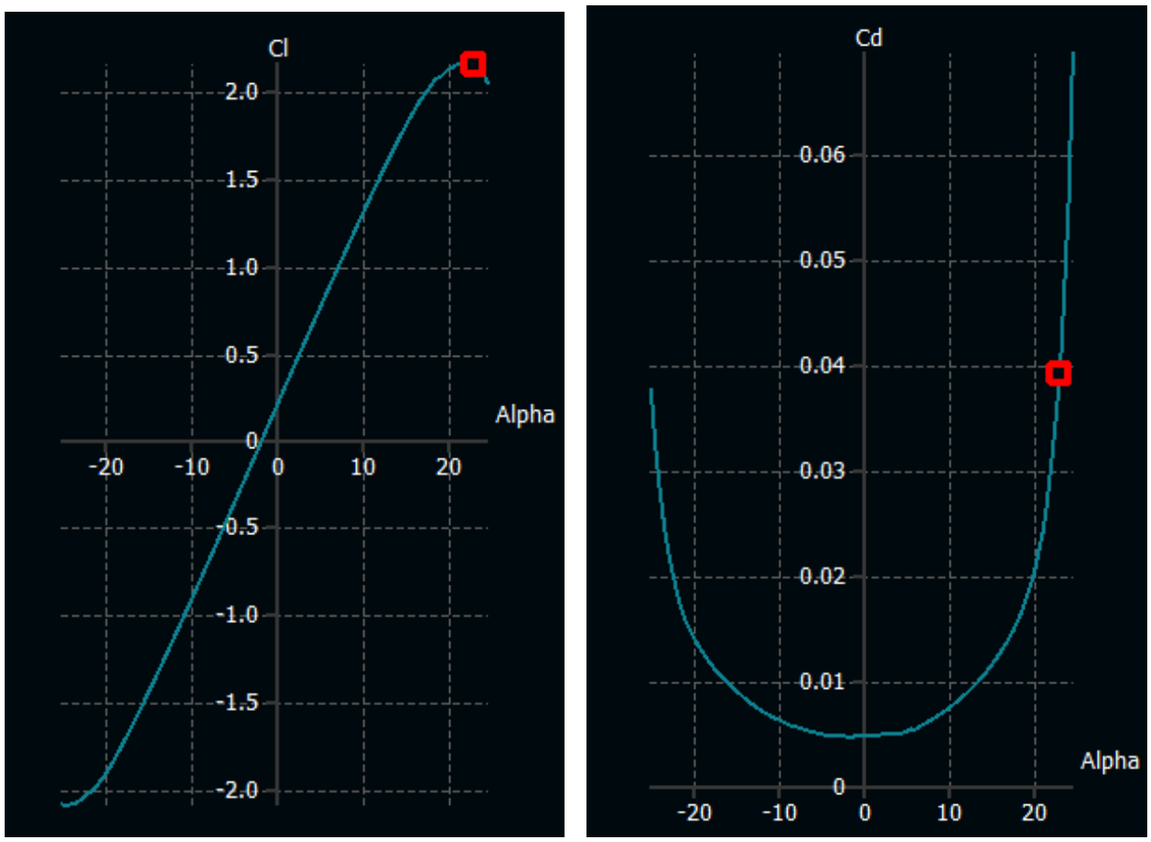

(a) Lift Coefficient With Varied Angle of Attack

(b) Viscous Drag Coefficient With Varied Angle of Attack

Figure 6.1: XFLR 5 Results (1) at Cruse Condition

Besides, the results the stall properties are also marked using a red square over every plot. From the data, the stall point seems to be angle of attack of 22.5 degrees where C_L peaks at 2.1 and then begins to drop. At that angle of attack, $C_D = 0.039$ and $C_M = 0.009$. Besides stall, the zero lift angle of attack is about -2 degrees and the lift coefficient for zero angle of attack is 0.2. Using the 2D thin airfoil theory, the zero lift angle of attack is -1.32 degrees which is close enough to the simulated data. Moreover, the coefficient of moment for zero angle of attack is -0.04 and that of thin airfoil theory is -0.03 which is also pretty close. Overall, the simulated 2D data matches the 2D data given by airfoil tools [1].

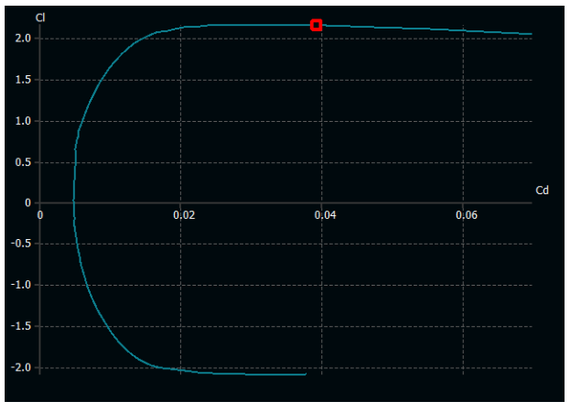

(a) Ratio of Lift and Drag Coefficient with Varied Angle of Attack

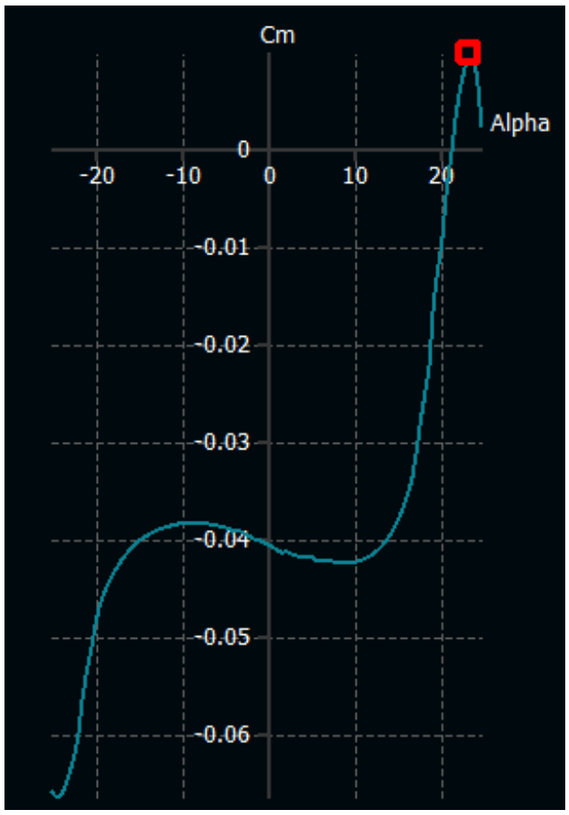

(b) Coefficient of Moment with Varied Angle of Attack

Figure 6.2: XFLR 5 Results (2) at Cruise Condition

7 Flaps and Slats

To prevent a high angle of attack while still generating high lift, slats and flaps are used as additional control surfaces on the wings. As shown in Figure 7.1, slats are situated at the front of the wing and flaps at the back. Actuation of either of these increases the camber of the wing and hence produces more lift for a smaller angle of attack. This is also the reason that these control surfaces are actuated during landing in order to reduce the speed of the airplane while still maintaining enough lift to prevent the craft from stalling.

Figure 7.1: Slats and Flaps for the Boeing 747-800

References

[1] *Airfoil database*, http://airfoiltools.com/airfoil/details?airfoil=bacxxx-il, Accessed: Insert Date Here.

[2] A. S. Exchange. "What is the exact wing chord length and thickness for boeing 747?" (year of publication (if available)), [Online]. Available: https://aviation.stackexchange.com/questions/82188/what-is-the-exact-wing-chord-length-and-thickness-for-boeing-747 (visited on 05/04/2024).

[3] "Boeing 747-8 design highlights," Boeing. (year of publication (if available)), [Online]. Available: https://www.boeing.com/commercial/747-8/design-highlights (visited on 05/04/2024).

[4] J. BAILEY. "How aircraft wings twist and why it's important." (2021), [Online]. Available: https://simpleflying.com/aircraft-wing-twist/ (visited on 03/09/2021).

[5] AeroCorner. "Boeing 747-8 vs 737-800: A detailed comparison." (year of publication (if available)), [Online]. Available: https://aerocorner.com/comparison/boeing-747-8-vs-737-800/ (visited on 05/04/2024).

[6] T. W. Experience. "How fast does a boeing 747 fly?" (2024), [Online]. Available: https://www.wrightexperience.com/how-fast-does-a-boeing-747-fly/ (visited on 03/05/2024).

[7] L. S. Jernell, "Performance estimate of a boeing 747-100 transport mated with an outsize cargo pod," NASA Langley Research Center, Tech. Rep., Feb. 1980.

[8] B. R. Munson, D. F. Young, and T. H. Okiishi, *Fundamentals of Fluid Mechanics*, 5th. Hoboken, NJ: Wiley, 2006.